 https://doi.org/10.1130/G45874.1

SUPPLEMENTARY MATERIAL

The role of permafrost on the morphology of an MIS 3 moraine from the southern Laurentide Ice Sheet

Elizabeth G. Ceperley*, Shaun A. Marcott, Lucas Zoet, J. Elmo Rawling III, and Susan Zimmerman

*Corresponding author: ceperley@wisc.edu

Laboratory methods

Samples underwent physical and chemical preparation at the University of Wisconsin-Madison Cosmogenic Isotope Laboratory using procedures modified from (Kohl and Nishiizumi, 1992). Samples were crushed and sieved to separate the 250-710 micron size fraction, magnetically separated, and etched in dilute HCl and HF/HNO_3 acid solutions. Chemical frothing was performed on all non-magnetic grains in order to separate quartz from feldspar. The remaining quartz grains were treated with additional HF/HNO_3 etches until the desired quartz purity was achieved. Quartz purity was measured by inductively coupled plasma optical emission spectroscopy at the University of Wisconsin-Madison Water Science and Engineering Laboratory.

Beryllium was isolated from quartz following procedures adapted from the University of Vermont Cosmogenic Nuclide Laboratory (Corbett et al., 2016). Samples were spiked with ^{9}Be carrier solution prepared from raw beryl (OSU White standard; ^{9}Be concentration of 251.6 ± 0.9 ppm). We used anion and cation exchange chromatography to separate Fe, Ti, Al, and isolate Be. BeOH was precipitated in a pH 8 solution. The BeOH gels were converted to BeO by heating to 900-1000 ^{o}C with a rapid incinerator, mixed with Nb powder, and packed into stainless steel cathodes for accelerator mass spectrometry (AMS) analysis.

All $^{10}Be/^{9}Be$ ratios were measured at GeoCAMS Laboratory at Lawrence Livermore National Laboratory (LLNL) and normalized to standard 07KNSTD3110, which has an assumed $^{10}Be/^{9}Be$ ratio of 2.85×10^{12} (Nishiizumi et al., 2007). Analytical uncertainties ranged from 1-3%. Sample ratios were corrected using batch-specific blank values, which ranged from 1.2×10^{-15} to 2.3×10^{-15} (n = 6). Concentrations in Table DR1 are corrected from batch-specific blanks.

Exposure age calculation

^{10}Be exposure ages (Figure 1, Table DR1) were calculated with online CRONUS-Earth exposure age calculator version 3 (http://hess.ess.washington.edu/math/index_dev.html; Balco et al., 2008) using the default global ^{10}Be production rate and a nuclide-dependent scaling of Lifton-Sato-Dunai (Lifton et al., 2014). Exposure ages were also calculated using the Northeast North America ^{10}Be production rate (Balco et al., 2009) and the CRONUS-Earth “Primary” ^{10}Be calibration data set (Borchers et al., 2016), but ages changed by <0.4%, within the range of analytical uncertainty. Due to isostatic rebound and subsidence, the elevation history of our samples has a relatively minor effect on the exposure age calculation (<1%), which leads us to report our ^{10}Be

exposure ages without elevation corrections. No corrections for snow shielding or erosion, but were accounted for within the geologic uncertainty of the age calculation. We use 2.65 g/cm^3 as the density of quartz.

Cosmogenic surface exposure data interpretation

Threeo exposure dates were excluded from the mean moraine calculation because of potential inheritance (italicized ages on Figure 1B). We make the fundamental assumption that the majority of the boulders reflect the timing of deposition (with random errors), but that some boulders will have non-random, geologic errors related to inheritance or exhumation problems, making the boulders anomalously older or younger than others. Geologic outliers are identified using chi-square statistics and frequency distribution curves. The chi-square test is used to test the null hypothesis that the error distribution of the population is statistically different than random noise. Samples are rejected until population errors appear random. The multi-modal nature of the frequency distribution curves agree with the chi-square analysis; the samples rejected during the chi-square analysis are the samples which form the secondary frequency maxima.

Landscape diffusion modeling

We use the following equation to approximate slope change over time:

$$\frac{\partial z}{\partial t} = D\frac{\partial^2 z}{\partial x^2}$$

Where D equals the diffusion coefficient for the following weathering scenarios:

Climate state	**Time (ka)**	**Duration (ka)**	**D (m^2 y^{-1})**
Permafrost	33-14	19	3.9 x 10^{-2}
Non-permafrost	14-0	14	1 x 10^{-3}

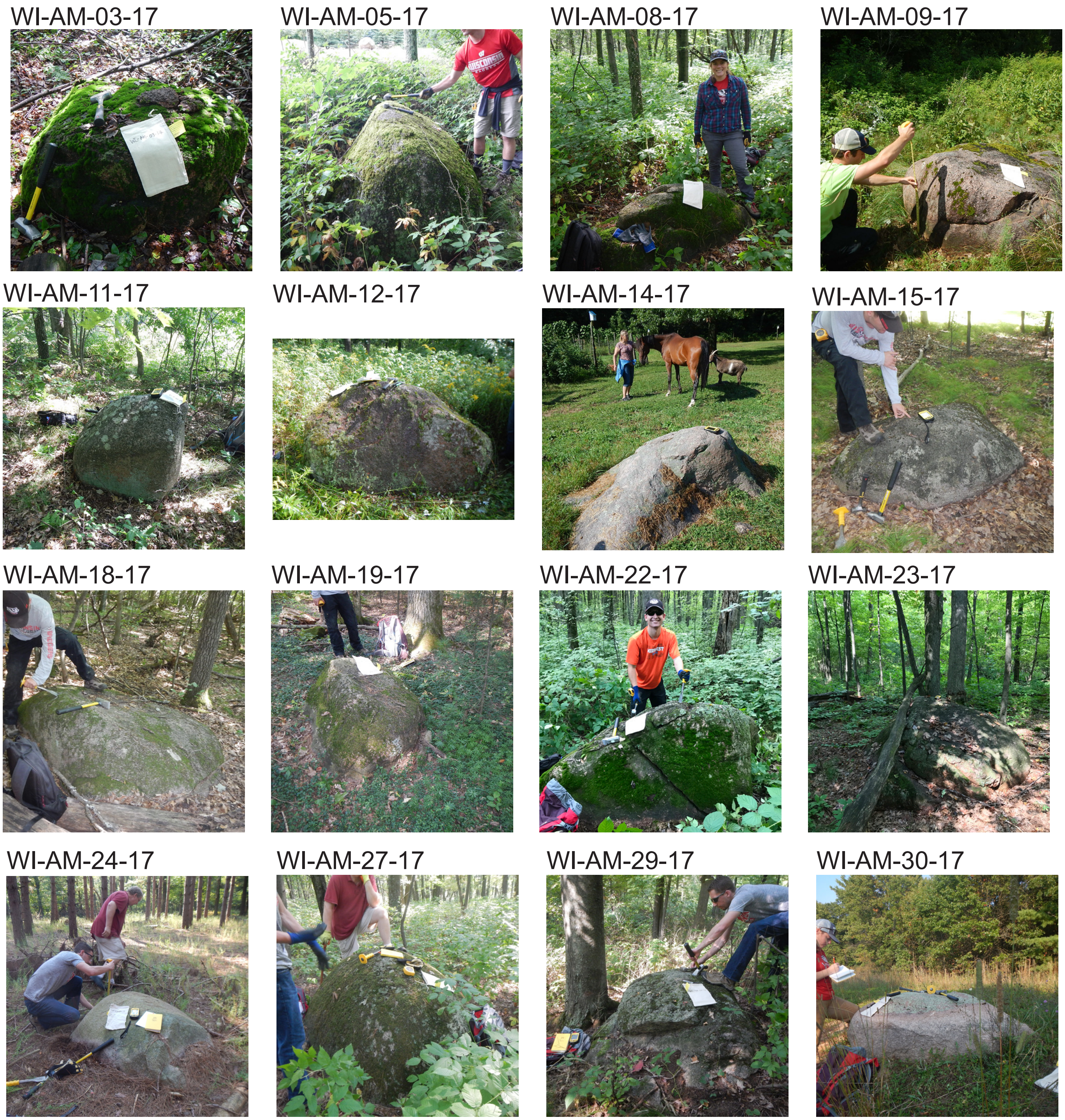

DR Figure 1. Photos of boulders sampled for ^{10}Be exposure dating on the Arnott and Almond Moraines, central Wisconsin. Refer to Table DR 1 for metadata and exposure age for each sample.

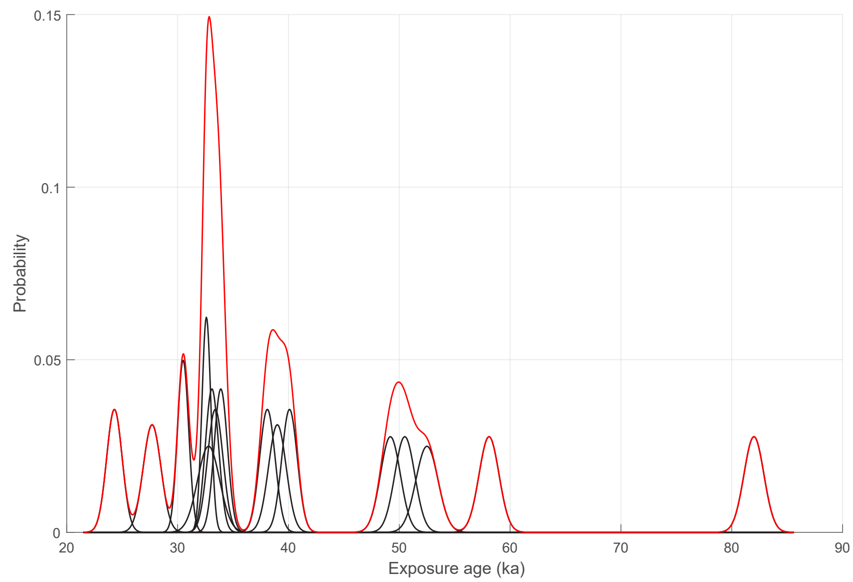

DR Figure 2. Probability distribution function of ^{10}Be ages from the Arnott Moraine, individual ages shown in black and cumulative curve in red.

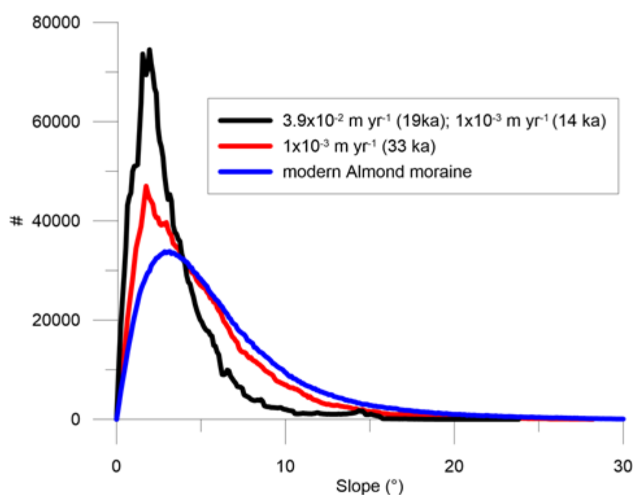

DR Figure 3. Histogram of relief for landscape diffusion model results with model runs with two different diffusion coefficients (red and black lines) and modern Almond Moraine relief (blue line).

Table DR1. Cosmogenic sample information

Sample[a]	Latitude (DD)	Longitude (DD)	Elevation (m asl)[b]	Shielding	Quartz (g)	^{9}Be carrier (μg)[c]	$^{10}Be/^{9}Be$ (10^{-15})[d]	1-sig (10^{-15})[e]	^{10}Be (atoms g^{-1})[f]	Unc. (atoms g^{-1})	^{10}Be age (ka)[g]
Almond Moraine											
WI-AL-01-17	44.4323	-89.3999	380	1	7.9655	193.1	67.93	2.10	1.07E+05	3.39E+03	19.7 ± 0.6
Arnott Moraine											
WI-AM-03-17	44.4483	-89.4673	350	1	24.3352	193.3	335.81	6.34	1.77E+05	3.37E+03	33.1 ± 0.6
WI-AM-05-17	44.3513	-89.4629	352	1	19.9351	193.9	431.74	8.14	2.79E+05	5.29E+03	52.5 ± 1.0
WI-AM-08-17	44.3555	-89.4699	356	1	45.0421	193.9	635.20	11.76	1.82E+05	3.38E+03	33.9 ± 0.6
WI-AM-09-17	44.4249	-89.4764	355	0.9988	46.3783	180.6	1186.57	19.21	3.08E+05	5.00E+03	58.1 ± 0.9
WI-AM-11-17	44.4246	-89.4749	355	1	19.5634	193.8	267.45	3.87	1.76E+05	2.56E+03	32.6 ± 0.4
WI-AM-12-17	44.3330	-89.4755	347	0.9633	45.1346	194.3	1451.28	16.08	4.17E+05	4.63E+03	82.0 ± 0.9
WI-AM-14-17	44.3362	-89.4725	356	1	44.9706	176.4	1010.86	18.83	2.64E+05	4.94E+03	49.2 ± 0.9
WI-AM-15-17	44.4557	-89.4748	350	1	45.0223	193.7	940.29	17.34	2.70E+05	4.98E+03	50.5 ± 0.9
WI-AM-18-17	44.3993	-89.4695	360	0.9970	45.0462	194.2	575.59	10.63	1.65E+05	3.06E+03	30.5 ± 0.5
WI-AM-19-17	44.4673	-89.4658	355	0.9903	45.2960	169.8	519.54	15.52	1.30E+05	3.89E+03	24.3 ± 0.7
WI-AM-22-17	44.4991	-89.4561	358	1	19.6835	193.6	230.14	6.99	1.50E+05	4.60E+03	27.7 ± 0.8
WI-AM-23-17	44.5010	-89.4545	355	1	13.8543	193.1	234.67	4.29	2.17E+05	3.99E+03	40.1 ± 0.7
WI-AM-24-17	44.3348	-89.4702	362	1	20.5826	192.8	290.49	6.08	1.81E+05	3.81E+03	33.4 ± 0.7
WI-AM-27-17	44.3413	-89.4680	369	1	15.7084	192.9	254.69	4.86	2.08E+05	3.99E+03	38.1 ± 0.7
WI-AM-29-17	44.3436	-89.4679	374	1	45.0455	194.0	746.05	15.11	2.14E+05	4.35E+03	39.0 ± 0.8
WI-AM-30-17	44.3936	-89.4685	358	1	7.7426	191.9	109.08	3.45	1.77E+05	5.71E+03	32.8 ± 1.0

[a]All samples were from granites, age calculations assume a quartz density of 2.65 g cm^{-3}, and have a thickness of 2.0 cm

[b]Sample locations were collected with a hand-held GPS (WGS84)

[c]Elevations were extracted from a 0.60 m resoltuion LiDAR elevation dataset for Portage Co (NAD83)

[d]OSU Blue ^{9}Be carrier was used for all samples, which has a concentration of 251.6 x 10^{-4} μg

[e]All AMS measurements are standardized to 07KNSTD

[f]1-sigma AMS uncertainty

[g] ^{10}Be atom concetrations are batch-specific blank-corrected (see supplemental text)

[h]All age calculations use standard atmosphere, modern elevation, zero erosion, and are presented with 1-sigma analytical uncertainty.

References

Balco, G., Briner, J., Finkel, R.C., Rayburn, J.A., Ridge, J.C., and Schaefer, J.M., 2009, Regional beryllium-10 production rate calibration for late-glacial northeastern North America: Quaternary Geochronology, v. 4, p. 93–107.

Balco, G., Stone, J.O., Lifton, N.A., and Dunai, T.J., 2008, A complete and easily accessible means of calculating surface exposure ages or erosion rates from ^{10}Be and ^{26}Al measurements: Quaternary Geochronology, v. 3, p. 174–195.

Borchers, B., Marrero, S., Balco, G., Caffee, M., Goehring, B., Lifton, N., Nishiizumi, K., Phillips, F., Schaefer, J., and Stone, J., 2016, Geological calibration of spallation production rates in the CRONUS-Earth project: Quaternary Geochronology, v. 31, p. 188–198.

Corbett, L.B., Bierman, P.R., and Rood, D.H., 2016, An approach for optimizing in situ cosmogenic ^{10}Be sample preparation: Quaternary Geochronology, v. 33, p. 24–34.

Kohl, C.P., and Nishiizumi, K., 1992, Chemical isolation of quartz for measurement of in-situ-produced cosmogenic nuclides: Geochimica et Cosmochimica Acta, v. 56, p. 3583–3587.

Lifton, N., Sato, T., and Dunai, T.J., 2014, Scaling in situ cosmogenic nuclide production rates using analytical approximations to atmospheric cosmic-ray fluxes: Earth and Planetary Science Letters, v. 386, p. 149–160.

Nishiizumi, K., Imamura, M., Caffee, M.W., Southon, J.R., Finkel, R.C., and McAninch, J., 2007, Absolute calibration of 10Be AMS standards: Nuclear Instruments and Methods in Physics Research Section B: Beam Interactions with Materials and Atoms, v. 258, p. 403–413.